

3D Raytracing through Homogeneous Anisotropic Layered Media with Smooth Interfaces

J. Costa, M. Schoenberg, and J. Urban

email: *jesse@ufpa.br*

keywords: *Raytracing, Anisotropy, Continuation Method*

ABSTRACT

Two-point raytracing problem is solved for events in a piecewise homogeneous and laterally varying 3D anisotropic media by continuation techniques. A combination with the shooting method allows to extend the method for computation of qS_1 and qS_2 events. The algorithm has the same performance and robustness as previous implementations of the continuation method for tracing rays in isotropic models. This simple routine has several useful applications. Firstly, an efficient forward problem solver in traveltimes inversion for elastic parameters in the presence of anisotropy. Secondly, the Newton-Raphson iterations during two-point raytracing produces the wavefront attributes, slowness and wavefront curvature. These quantity allows the computation of geometrical spreading and second order approximations for traveltimes, as required in CRS. Therefore the effects of anisotropy on CRS, in simple velocity models, can be investigated.

INTRODUCTION

A computational scheme is proposed to solve two-point raytracing, in a piecewise homogeneous and laterally varying 3D anisotropic layered media, based on the continuation method. The algorithm is an extension to the anisotropic case of previous works for isotropic media (Keller and Perozzi (1983); Docherty and Bleistein (1984)).

The continuation method permits to trace rays through a complex model by continuous transformations from simpler intermediary configurations. This procedure warrant robustness to the iterative techniques used to solve the nonlinear system of equations that arises from Fermat's principle. A sequence of continuation steps is performed. Starting with a vertical ray in an isotropic layered medium, the isotropic slowness surfaces are deformed to the intended anisotropic slowness surfaces at each layer. The next step is to transform the flat interfaces to the desired curved ones. Finally we move source and receiver positions to the configuration we want to achieve.

The algorithm has the same performance described by Docherty and Bleistein (1984) for isotropic models when computing qP raypaths. The computation of qS_1 and qS_2 raypaths presents difficulties at the singular regions where the slowness surfaces for these waves intersects one another and regions where they are not convex. A shooting approach can remedy most of these problems, but the performance degrades if many restarts are required.

This procedure is well adapted to compute raypath and traveltimes for surface seismics and VSP experiments in anisotropic models. The algorithm can be a forward problem routine for a traveltimes inversion scheme which produces estimatives of the elastic constants structure for subsurface, most like the works of Whitmore and Lines (1986), Chiu and Stewart (1987) and Guiziou and Haas (1988), without the limitations of the elliptical anisotropy assumption. Other possible applications include VSP-CDP mapping and the computation of wavefront attributes, slowness vector and wavefront curvature, along the raypath.

FERMAT'S PRINCIPLE AND RAYPATH COMPUTATION

We assume a piecewise homogeneous, anisotropic, layered medium where the interfaces are described by functions

$$\phi(\mathbf{x}) = x_3 - \zeta(x_1, x_3) = 0 ,$$

where x_j represents Cartesian coordinates. The two-point raytracing problem in layered anisotropic medium through N layers can be stated, by Fermat's principle, as the following variational problem in phase space,

$$\text{Minimize}_{x_1^\alpha, x_2^\alpha, \mathbf{s}^\alpha} \quad \tau = \sum_{\alpha=1}^N s_j^\alpha \Delta x_j^\alpha \quad (1)$$

subjected to,

$$\mathcal{H}^\alpha(\mathbf{s}^\alpha) = 0, \quad \alpha = 1, \dots, N, \quad (2)$$

where, τ is the traveltime along the ray,

$$\Delta x_j^\alpha = x_j^\alpha - x_j^{\alpha-1},$$

$\mathbf{x}^\alpha = (x_j^\alpha)$ represents the ray intersection with the α -th interface,

$\mathbf{x}^0 = (x_j^0)$ is the source position,

$\mathbf{x}^N = (x_j^N)$ is the receiver position,

$\mathbf{s}^\alpha = (s_j^\alpha)$ is the slowness vector at the α -th layer,

$\mathcal{H}^\alpha(\mathbf{s}^\alpha)$ = is the dispersion relation at the α -th layer. Summation convention is assumed on subscript index j which identifies the cartesian coordinates directions.

Equation (1) arises from the relations (Musgrave (1970)),

$$\tau = \int_{ray} \mathbf{s} \cdot d\mathbf{x} = \int_{ray} \mathbf{s} \cdot \mathbf{v} d\tau = \int_{ray} d\tau . \quad (3)$$

Here \mathbf{s} is the slowness, \mathbf{v} is the group velocity and τ traveltime along the ray. The last identity results from the polar reciprocal relationship between slowness and group velocity $\mathbf{s} \cdot \mathbf{v} \equiv 1$. For a piecewise homogeneous layered media equation (3) reduces to (1).

The solution of (1) subject to (2) is straightforward using Lagrange multipliers,

$$\text{Minimize}_{x_1^\alpha, x_2^\alpha, \mathbf{s}^\alpha, \lambda^\alpha} \quad \tau = \sum_{\alpha=1}^N s_j^\alpha \Delta x_j^\alpha + \lambda^\alpha \mathcal{H}^\alpha(\mathbf{s}^\alpha) . \quad (4)$$

following standard procedures we obtain the nonlinear system of $5N + 3$ equations on $5N + 3$ unknowns, namely, $x_1^\alpha, x_2^\alpha, s_1^\alpha, s_2^\alpha, s_3^\alpha$:

$$\begin{aligned} \Phi_1^\alpha &= \Delta s_1^\alpha + \Delta s_3^\alpha \partial_1 \zeta^\alpha = 0 , \\ \Phi_2^\alpha &= \Delta s_2^\alpha + \Delta s_3^\alpha \partial_2 \zeta^\alpha = 0 , \\ \Phi_3^\alpha &= \Delta x_1^\alpha \partial_{s_3^\alpha} \mathcal{H}^\alpha - \Delta x_3^\alpha \partial_{s_1^\alpha} \mathcal{H}^\alpha = 0 , \\ \Phi_4^\alpha &= \Delta x_2^\alpha \partial_{s_3^\alpha} \mathcal{H}^\alpha - \Delta x_3^\alpha \partial_{s_2^\alpha} \mathcal{H}^\alpha = 0 , \\ \Phi_5^\alpha &= \mathcal{H}^\alpha(\mathbf{s}^\alpha) = 0 , \end{aligned} \quad (5)$$

These five equations express the basic geometrical relations for rays and slownesses through a homogeneous layered medium. Equations for Φ_1^α and Φ_2^α can be written as

$$(\mathbf{s}^{\alpha+1} - \mathbf{s}^\alpha) \times \mathbf{n}^\alpha = \mathbf{0} , \quad (6)$$

where \mathbf{n}^α is the unit vector normal to the α -th interface. This equation is a statement of the Snell's law. It requires that the variation of the slowness vector across an interface be parallel to the interface normal, i.e., tangential slowness component is continuous across the interface. Equations for Φ_3^α and Φ_4^α , express the relation between ray direction and slowness surface, and can be written as

$$(\mathbf{x}^\alpha - \mathbf{x}^{\alpha-1}) \times \nabla_{\mathbf{s}} \mathcal{H}^\alpha = \mathbf{0} , \quad (7)$$

this equation states that ray direction should be normal to the slowness surface. The last equation for Φ_5 , defines the slowness surfaces at each layer. The system of equations (5) in vector notation is,

$$\Phi(\mathbf{u}) = \mathbf{0}, \quad (8)$$

where,

$$\begin{aligned} \Phi^T &= (\phi_1^1, \dots, \phi_5^1, \dots, \phi_1^N, \dots, \phi_5^N, \phi_3^{N+1}, \phi_4^{N+1}, \phi_5^{N+1}), \\ \mathbf{u}^T &= (x_1^1, x_2^1, \dots, x_1^N, x_2^N, s_1^1, s_2^1, s_3^1, \dots, s_1^N, s_2^N, s_3^N). \end{aligned}$$

The system (8) can be solved iteratively using Newton-Raphson method. At the K -th iteration this corresponds to:

1. solve

$$\Delta \mathbf{u}^{(K)} \cdot \nabla_{\mathbf{u}} \Phi = -\Phi(\mathbf{u}^{(K)}) \quad \text{for } \Delta \mathbf{u},$$

2. update

$$\mathbf{u}^{(K+1)} = \mathbf{u}^{(K)} + \Delta \mathbf{u}^{(K)}, \quad (9)$$

CONTINUATION METHODS

Continuation techniques are used to solve the system (8) in order to add robustness to the Newton-Raphson iterations (9). The continuation method consists in solving the following nonlinear equation

$$\Phi(\mathbf{u}, \gamma) = \mathbf{0}, \quad (10)$$

instead of (8).

The parameter γ is intended to control the smooth transformation from problem $\Phi(\mathbf{u}, 0) = \mathbf{0}$, whose solution can be readily found, to $\Phi(\mathbf{u}, 1) = \Phi(\mathbf{u})$, which is the problem to be solved.

The solution of the two-point raytracing in 3D layered anisotropic medium can be constructed imbedding a sequential application of the continuation technique for the solution of (8).

Continuation of slowness surfaces For each layer, the dispersion relation may be written in the form

$$\mathcal{H}^\alpha(\mathbf{s}) = \gamma \mathcal{H}_{anis}^\alpha + (1 - \gamma) \mathcal{H}_{iso}^\alpha \quad i = 1, \dots, N, \quad (11)$$

where $\mathcal{H}_{anis}^\alpha$ and \mathcal{H}_{iso}^α are the dispersion relations for the anisotropic layers and for initial isotropic layers, respectively. The starting layered isotropic model ($\gamma = 0$), has compressional velocities $\alpha_i^2 = \max(a_{11}, a_{22}, a_{33})$, at each layer, where a_{IJ} are the density normalized elastic moduli in condensed notation (Musgrave (1970)).

Beginning with a vertical ray in the initial flat layered isotropic model, so $\mathbf{u}(\gamma = 0)$ is trivially computed, the algorithm proceeds as follows. The initial guess for Newton iterations (9) for a new $\gamma = \gamma + \Delta\gamma$ is computed (Docherty and Bleistein (1984)):

1. solve

$$\frac{d\Phi}{d\gamma} = \frac{d\mathbf{u}}{d\gamma} \cdot \nabla_{\mathbf{u}} \Phi + \Phi, \gamma = \mathbf{0} \quad \text{for } \frac{d\mathbf{u}}{d\gamma}, \quad (12)$$

2. start Newton iterations from

$$\mathbf{u}^0(\gamma + \Delta\gamma) = \mathbf{u}(\gamma) + \frac{d\mathbf{u}}{d\gamma} \Delta\gamma. \quad (13)$$

Then iterate using Newton-Raphson equations (9). If the Newton method does not converge in 5 iterations, halve $\Delta\gamma$ and start again. After convergence double the value $\Delta\gamma$ and continue in the same way until $\gamma = 1$. Usually, we can go from $\gamma = 0$ to $\gamma = 1$ in one step $\Delta\gamma = 1$. When $\gamma = 1$, the model is the desired set of anisotropic layers with flat interfaces.

Continuation of interfaces The next step is to deform the interfaces from flat layers to the desired ones keeping source and receiver vertically aligned. This is done using,

$$x_3^\alpha = h^\alpha + \gamma \zeta^\alpha(x_1, x_2), \quad (14)$$

so, when $\gamma = 0$, the interfaces are flat, and, when $\gamma = 1$, the desired interfaces are achieved. The interfaces are defined by specifying a set of points $\zeta(x_1, x_2)$ over a grid for each interface. B-spline interpolation are used to define the interfaces and evaluation of the required derivatives.

The procedure follows as before. The starting values for Newton iterations is computed similarly from

$$\frac{d\Phi}{d\gamma} = \frac{d\mathbf{u}}{d\gamma} \cdot \nabla_{\mathbf{u}} \Phi + \Phi, \gamma = 0, \quad (15)$$

and

$$\mathbf{u}^0 = \mathbf{u} + \frac{d\mathbf{u}}{d\gamma} \Delta\gamma, \quad (16)$$

where $\mathbf{u}(\gamma = 0)$ is the solution of the slowness continuation procedure.

Receiver and Source continuation Now that the intended media structure was achieved, the next step is to move the receiver to the desired configuration applying the continuation procedure to the relation,

$$\mathbf{x}_{rec} = \gamma \mathbf{x}_{rec}^{new} + (1 - \gamma) \mathbf{x}_{rec}^{old}, \quad (17)$$

where $\mathbf{x}_{rec} = (x_{rec}, y_{rec}, z_{rec})$. Here $\gamma = 0$ means a previous computed receiver position and $\gamma = 1$ the new receiver position for raypath computation.

The starting guess for Newton iterations comes from the solution of

$$\frac{d\Phi}{d\gamma} = \frac{d\mathbf{u}}{d\gamma} \cdot \nabla_{\mathbf{u}} \Phi + \frac{d\mathbf{x}_{rec}}{d\gamma} \cdot \nabla_{\mathbf{x}_{rec}} \Phi = 0, \quad (18)$$

with

$$\mathbf{u}^0 = \mathbf{u} + \frac{d\mathbf{u}}{d\gamma} \Delta\gamma, \quad (19)$$

here $\mathbf{u}(\gamma = 0)$ is the solution for the previous receiver position. The same procedure is applied for source continuation. The corresponding expressions can be obtained just changing the labels of receiver position for the source position at the above equations.

SHOOTING STILL REQUIRED

Two-point raytracing has its drawbacks, though. Firstly, Newton-Raphson iterations fail when matrix $\nabla_{\mathbf{u}} \Phi$ is singular. This occurs in several instances during raytracing: over an interface saddle point, if ray is tangent to an interface, or when receivers are at shadow zones. Secondly, when more than one ray connects source and receiver, two-point raytracing converges to a single trajectory depending on initial guess, in other words, only a single branch of travelttime surface is computed and the method fails at the borders of these branches. To overcome these problems the algorithm has to be combined with a shooting strategy (Press et al. (1989)). Whenever Newton iterations fail a ray is computed using the shooting algorithm. Since raypath is a straight line in each layer, raytracing is reduced to compute the intersection of the ray with the interfaces and apply Snell's law to proceed across an interface until we reach the layer containing the receivers. Once a new ray is successfully computed in the neighborhood of a singular point, two-point raytracing can be tried again to compute rays to nearby receivers. If the ray identifies a shadow zone the procedure is interrupted.

NUMERICAL RESULTS

The algorithm was applied to compute raypaths for a model consisting of five layers, having strongly anisotropic elastic properties, separated by smooth interfaces. The density normalized elastic parameters

for each layer are presented in appendix A. The layers are indexed from 1 to 5 from top to bottom. The qP group velocity surface for each medium are shown in Figure 1, Figure 2 and Figure 3.

We only present computation of rays associated with qP events, although qS events can be computed if a initial ray is determined using the shooting method. Figures 4(a) and 4(b) show the result of raypath computation for receivers along a line in the surface. The raypaths include a multiple in the third layer.

The second example, Figure 5, includes an unusual configuration of source and receivers at the surface just to point out the possibilities of this implementation. Again a multiple was computed in the third layer. The third example, Figure 6, has the same distribution of receivers at the surface but now the source is located in the third layer as in a reverse 3-D VSP experiment.

One can always find complex models, which present shadow zones or rough interfaces, where Newton iterations fail and many restarts using the shooting method are required. This algorithm is not well suited for these models. For applications which do not require such complex models and where qP waves are the main concern the algorithm is quite efficient.

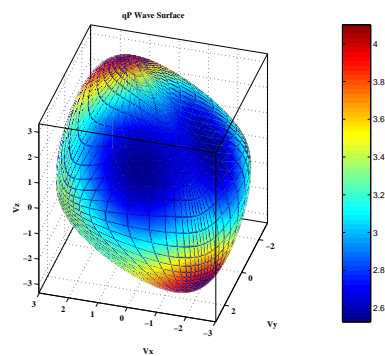


Figure 1: qP Wave Surface for layer 1. This is a tilted orthorhombic medium. The velocity components are in km/s and the colors represent the group speed also in km/s.

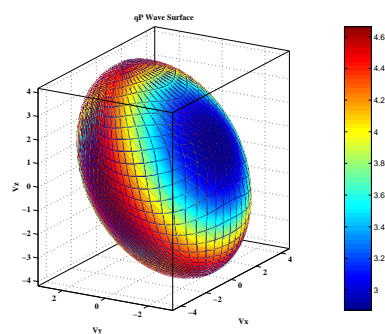


Figure 2: qP Wave Surface for layers 2 and 4. This is a tilted TI medium. The velocity components are in km/s and the colors indicate the group speed in km/s.

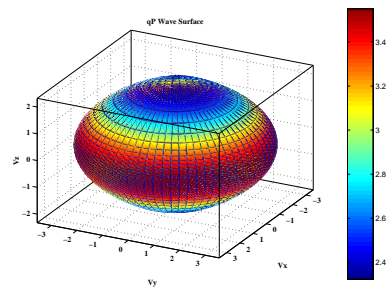


Figure 3: qP Wave Surface for layer 3 and layer 5. This is also a tilted TI medium. The velocity components are in km/s and the colors represent the group speed in km/s.

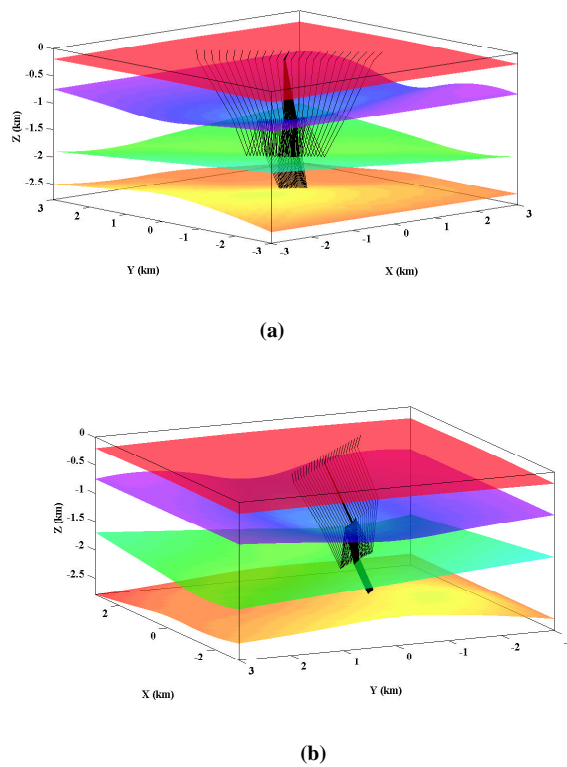


Figure 4: Two views for qP raypaths for receivers along a line in the surface. Note the multiple in layer 3.

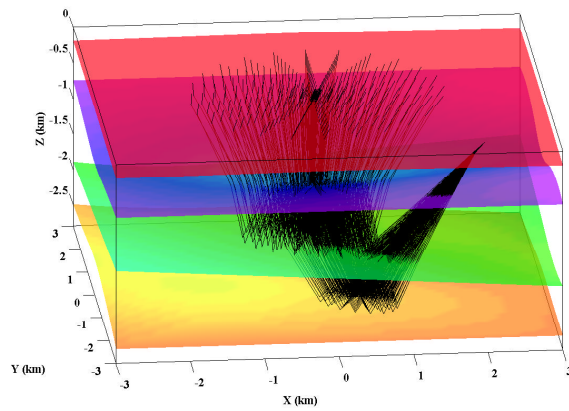
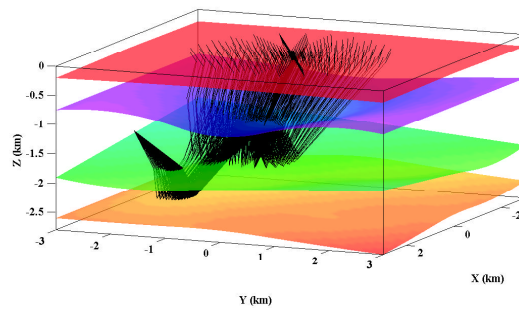
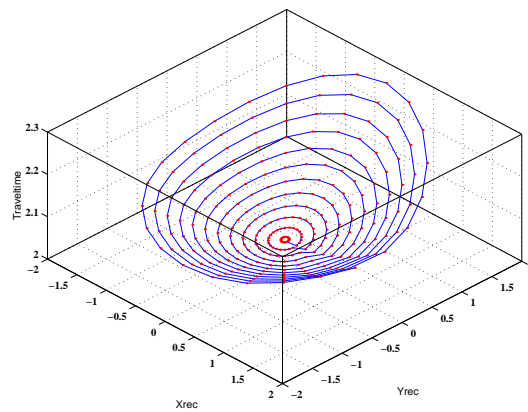


Figure 5: Rays for a complex 3-D surface acquisition geometry.



(a) Rays for 3-D VSP .



(b) Traveltimes in seconds .

Figure 6: Rays and traveltimes for an multiazimuthal 3-D VSP acquisition geometry.

CONCLUSION

An extension of the continuation method proposed by Keller & Perozzi (1983) to anisotropic models in 3-D was developed. The algorithm is efficient when computing qP events. The computation of the qS_1 and qS_2 trajectories requires the use of shooting method to find, besides the starting ray, new initial approxi-

mations whenever two-point raytracing fails due to singular regions in the associated slowness surface or other possible causes. Although the algorithm do not handle general inhomogeneous anisotropic models, it allows a simple model specification for interfaces and arbitrary anisotropy. The performance of the algorithm permits its application to procedures requiring the computation of a large number of raypaths, as on inversion algorithms and VSP-CDP mapping in 3-D. It can also be helpful, when wavefront attributes as slowness vector and wavefront curvature are required as occurs in geometrical spreading computations or in CRS studies.

ACKNOWLEDGEMENTS

This work was kindly supported by the sponsors of the *Wave Inversion Technology (WIT) Consortium*, Karlsruhe, Germany.

REFERENCES

- Chiu, S. and Stewart, R. (1987). Tomographic determination of three- dimensional seismic velocity structure using well logs, vertical seismic profiles, and surface seismic data. *Geophysics*, 52(8):1085–1098.
- Docherty, P. and Bleistein, N. (1984). A fast ray tracing routine for laterally inhomogeneous media. *Presented at 54th Annual SEG Meeting, Atlanta*.
- Guiziou, J. and Haas, A. (1988). Three dimensional inversion in anisotropic media. *Presented at 58th Annual SEG Meeting, Anaheim*.
- Keller, H. and Perozzi, D. (1983). Fast seismic ray tracing. *SIAM J. Appl. Math.*, 43:981–992.
- Musgrave, M. (1970). *Crystal Acoustics*. Holden-Day, London.
- Press, W., Flannery, B., Teukolsky, S., and Vetterling, W. (1989). *Numerical Recipes the art of scientific computing*. Cambridge University Press, Cambridge.
- Whitmore, N. and Lines, L. (1986). Vertical seismic profiling depth migration of a salt dome flank. *Geophysics*, 51(5):1087–1109.

APPENDIX A

The density normalized elastic tensor for the three different materials forming the layers in the model used for numerical test. The units are in $(km/s)^2$.

Layer 1 (orthorhombic):

$$\mathbf{A}_1 = \begin{bmatrix} 8.637 & 4.867 & 3.238 & -0.626 & 1.559 & 0.452 \\ & 8.637 & 3.238 & -1.559 & 0.626 & 0.452 \\ & & 10.198 & -1.690 & 1.690 & -0.835 \\ & & & 3.388 & -1.503 & 0.598 \\ & & & & 3.388 & -0.598 \\ & & & & & 4.350 \end{bmatrix}$$

Layers 2 and 4 (TI):

$$\mathbf{A}_2 = \begin{bmatrix} 21.750 & 3.635 & 5.166 & 1.326 & 0.000 & 0.000 \\ & 9.326 & 5.169 & 1.596 & 0.000 & 0.000 \\ & & 16.076 & 4.250 & 0.000 & 0.000 \\ & & & 5.299 & 0.000 & 0.000 \\ & & & & 6.682 & 2.126 \\ & & & & & 4.227 \end{bmatrix}$$

Layers 3 and bottom medium (TI) :

$$\mathbf{A}_3 = \begin{bmatrix} 12.600 & 3.254 & 1.361 & 0.000 & 0.000 & 0.000 \\ & 12.600 & 1.361 & 0.000 & 0.000 & 0.000 \\ & & 5.400 & 0.000 & 0.000 & 0.000 \\ & & & 2.250 & 0.000 & 0.000 \\ & & & & 2.250 & 0.000 \\ & & & & & 4.673 \end{bmatrix}$$